

# Direct reduction of SO<sub>2</sub> to elemental sulfur by methane over ceria-based catalysts

Tianli Zhu, Andreas Dreher<sup>1</sup>, Maria Flytzani-Stephanopoulos\*

*Department of Chemical Engineering, Tufts University, Medford, MA 02155, USA*

Received 31 July 1998; received in revised form 18 January 1999; accepted 3 February 1999

## Abstract

The catalytic reduction of SO<sub>2</sub> to elemental sulfur by methane was studied over ceria-based catalysts. Both La-doped and undoped ceria were found to catalyze the SO<sub>2</sub> reduction by CH<sub>4</sub> in the temperature range of 550–750°C at atmospheric pressure and with feed gases containing a molar ratio of CH<sub>4</sub>/SO<sub>2</sub> = 0.5–3. At temperatures below ~550°C, the catalyst surface is capped by SO<sub>2</sub>. The reaction light-off coincides with the threshold temperature for sulfate decomposition. Various SO<sub>2</sub>/CH<sub>4</sub>/H<sub>2</sub>O gas mixtures were used to study the catalyst activity and selectivity to elemental sulfur. The incorporation of nickel and copper improves the wet activity of Ce(La)Ox catalysts. Also, the addition of a low amount (5 at.%) of copper or nickel into La-doped ceria, Ce(La)Ox, had a markedly different effect on the catalyst selectivity under fuel-rich conditions. The Cu–Ce(La)Ox catalyst has higher selectivity to elemental sulfur and complete oxidation products (H<sub>2</sub>O, CO<sub>2</sub>), while Ni–Ce(La)Ox favors the formation of H<sub>2</sub>S and partial oxidation products (CO). The catalyst activity/selectivity studies were complemented by SO<sub>2</sub> uptake experiments and by reduction of the as-prepared and pre-sulfated catalysts in methane, both isothermally and in the TPR mode. The initial rate of reduction of pre-sulfated catalysts with methane is similar for Ce(La)Ox, Cu–Ce(La)Ox and Ni–Ce(La)Ox in the temperature range of 500–700°C. Activation of methane on these surfaces requires partial sulfate decomposition. ©1999 Elsevier Science B.V. All rights reserved.

**Keywords:** Elemental sulfur recovery; Catalytic sulfur dioxide reduction; Methane-TPR; Copper and cerium oxide; Nickel and cerium oxide; SO<sub>2</sub> uptake

## 1. Introduction

Over the past several decades, SO<sub>2</sub> emission standards have become ever more stringent. The most recent amendments to the Clean Air Act (1990) set a cap of total SO<sub>2</sub> emissions from US utilities at ~9MT per year. Much stricter sulfur emission con-

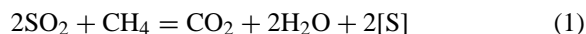
trol is also being applied to industrial boilers and other sources. Commercial sulfur control technologies typically use wet scrubbing systems based on limestone, lime or sodium carbonate for flue gas desulfurization (FGD). The large amount of solid waste generated from these processes is a potential environmental problem and its disposal entails continuously increasing landfill costs. Regenerative FGD processes are considered the most promising alternative sulfur removal technologies, having several advantages such as energy efficiency and no waste to dispose off. The regeneration off-gas is a sulfur dioxide-rich stream that

\* Corresponding author. Tel.: +1-617-627-3048; fax: +1-617-627-3391; e-mail: mstephanopoulos@infonet.tufts.edu

<sup>1</sup> Present address: Institute of Energy Engineering, Technical University of Berlin, Germany

needs to be converted to elemental sulfur or sulfuric acid for sulfur recovery. Treatment of this regeneration off-gas is integrally related to the regenerative FGD processes. Single-stage catalytic reduction of SO<sub>2</sub> to elemental sulfur is a promising sulfur recovery approach that may also have economic benefits from the sale of sulfur, a safe material to handle, transport and store. Its success will accelerate the commercialization of regenerative FGD processes.

Several reductants, including carbon monoxide, hydrogen, syngas and methane have been examined for SO<sub>2</sub> reduction. Methane is an attractive reductant, due to abundant and cheap natural gas. The reaction between sulfur dioxide and methane has been studied since the beginning of this century [1]. The primary overall reaction is:



where [S] represents the various elemental sulfur forms (S<sub>2</sub>, S<sub>6</sub>, S<sub>8</sub>). A number of side reactions and intermediate products are, in general, possible in the SO<sub>2</sub> + CH<sub>4</sub> system. Byproducts, such as H<sub>2</sub>S, COS, CS<sub>2</sub>, CO and H<sub>2</sub>, can be formed under certain conditions. The catalysts previously studied for this reaction include bauxite [2], alumina [3], transition metal sulfides [4,5], and alumina-supported catalysts [6–9]. Several recent studies have focused on supported molybdenum sulfide catalysts with concentrated SO<sub>2</sub> gas mixtures [5,7,8]. These have shown that a molybdenum content higher than 15 wt.% is necessary for a high catalyst activity irrespective of the type of support. This was attributed to the formation of MoS<sub>2</sub> crystal cluster on the support surface [7]. Cobalt oxide was recently reported as an active catalyst over alumina [9], but only at high temperatures (700–820°C). CoS<sub>2</sub>, identified by XRD in the used sample, was thought to be the active phase for the reaction between SO<sub>2</sub> and CH<sub>4</sub>. That the mechanism involves formation of [S] via intermediate H<sub>2</sub>S [8] seems to be a reasonable conclusion for these catalysts, since MoS<sub>2</sub> and CoS<sub>2</sub> are active catalysts for the H<sub>2</sub>S decomposition [10–12], while alumina itself is active for the Claus reaction. Because sulfur is a secondary product over these catalysts, the sulfur yield is maximized at very low space velocity. The optimized ratio of SO<sub>2</sub>/CH<sub>4</sub> used by various authors [5,6,13] is typically higher than the stoichiometric ratio of 2 : 1 (Reaction

(1)) to shift the activity to a lower temperature, albeit at the expense of selectivity to elemental sulfur.

A different reaction mechanism is displayed over cerium oxide-based catalysts. We have recently reported that the SO<sub>2</sub> reduction by CO on ceria-based catalysts follows the redox mechanism [14–16]. Accordingly, CO creates surface oxygen vacancies that are taken up by SO<sub>2</sub>, which is thereby reduced to elemental sulfur. Sulfur is, thus, a primary product, and very high space velocity can be used without affecting the sulfur yield.

In this paper, we report on the catalytic activity/selectivity of ceria-based catalysts for the reduction of SO<sub>2</sub> by CH<sub>4</sub> at a relatively high space velocity of 20,000–40,000 h<sup>-1</sup> (STP). The catalyst performance was addressed in parametric studies, which also included the effect of catalyst composition. The properties of ceria-based catalysts for this reaction were examined by isothermal SO<sub>2</sub> uptake and reduction studies of the as-prepared and pre-sulfated catalysts in methane.

## 2. Experimental

### 2.1. Catalyst preparation and characterization

Bulk catalysts were prepared by the urea gelation/coprecipitation method using metal nitrates and urea [17]. This method provides well-dispersed and homogeneously mixed metal oxides. The preparation process consists of the following steps: (i) mixing nitrate salts of metals with urea and heating the solution to 100°C under continuous stirring; (ii) after coprecipitation, boiling the resulting gels vigorously for 8 h; (iii) filtering and washing the precipitate twice with hot deionized water; (iv) drying the precipitate overnight in a vacuum oven at 110°C; (v) crushing the dried lumps into powder and calcining in static air for 3 h at 650°C. The typical surface area of the thus prepared CeO<sub>2</sub>-based catalysts was in the range of 75–120 m<sup>2</sup> g<sup>-1</sup>, as shown in Table 1. The samples used in the SO<sub>2</sub> and CH<sub>4</sub> reaction tests were further heated at 720°C for 3 h (surface area 45–70 m<sup>2</sup> g<sup>-1</sup>). The packing density of the thus prepared catalysts was around 1.8–2 g cm<sup>-3</sup>. The pore volume of the catalysts was measured by adding deionized water dropwise on a specific amount of catalyst up to the

Table 1  
Properties of catalysts tested in this work

Sample <sup>a</sup>	Surface area (m <sup>2</sup> g <sup>-1</sup> )			Surface composition <sup>b</sup>		
	650°C calcined <sup>c</sup>	720°C calcined <sup>c</sup>	750°C calcined <sup>c</sup>	Ce	La (at.%)	Metal
CeO <sub>2</sub>	75	45	40			
Ce(4.5% La)Ox	90	71	59			
Ce(10% La)Ox	106	70	64			
Ce(20% La)Ox	120		58			
5%Cu–Ce(4.5% La)Ox	89	65		77.7	3.9	18.4
5%Ni–Ce(4.5% La)Ox (6.0 at.% La, 4.7 at.% Ni) <sup>d</sup>	99	52	42	94.6	2.1	3.2
10% Ni–Ce(4.5% La)Ox (5.7 at.% La, 9.4 at.% Ni) <sup>d</sup>	89	49	43	87.9	6.0	6.1

<sup>a</sup> Prepared by the urea gelation/coprecipitation method [17].

<sup>b</sup> Determined by XPS of the 720°C air-calcined samples.

<sup>c</sup> In static air for 3 h.

<sup>d</sup> Analyzed by ICP.

onset of ‘beading’. For the materials reported in this work, the pore volume was about 0.10 cm<sup>3</sup> g<sup>-1</sup>.

The total catalyst surface area was measured by single-point N<sub>2</sub> adsorption/desorption on a Micromeritics Pulse ChemiSorb 2705 instrument. For bulk composition analysis, the catalyst powder was dissolved in a 70% HNO<sub>3</sub> acid solution (ACS reagent) and diluted with deionized water. The resulting solution was analyzed by inductively coupled plasma (ICP) atomic emission spectrometry (Perkin Elmer Plasma 40). X-ray power diffraction (XRD) analysis of catalysts was performed on a Rigaku 300 instrument with rotating anode generator and monochromatic detector. A Cu K $\alpha$  radiation was used with a power setting of 60 kV and 300 mA. The typical operation parameters were: divergence slit of 1°, scattering slit 1°, receiving slit 0.15°, and a scan rate of 1° min<sup>-1</sup> with 0.02° data interval. The catalyst surface composition was determined by X-ray photoelectron spectroscopy (XPS) on a Perkin Elmer 5100C system. All measurements were carried out at room temperature and without any sample pretreatment. A Mg K $\alpha$  X-ray source was primarily used in this work. The X-ray source was typically set at 15 kV and 20 mA.

### 3. Apparatus and procedures

#### 3.1. Catalyst performance evaluation

Catalyst activity tests were conducted in a laboratory-scale, packed-bed flow reactor made of

quartz (ID = 10 mm) with a porous quartz frit supporting the catalyst. All catalysts were in powder form (<150  $\mu$ m). Typically, 150 mg catalyst was loaded in the reactor for activity tests, and the contact time was 0.18–1.08 g s cm<sup>-3</sup>. The contact time is defined as the ratio of the amount of catalyst used for reaction (g) to the inlet flow rate (cm<sup>3</sup> s<sup>-1</sup>) (STP). This is, thus, equal to the reciprocal of space velocity times the catalyst density. The reactor was heated inside a Lindberg electric furnace. The temperature was measured by a quartz tube-sheathed K-type thermocouple placed at the top of the packed bed, and was controlled by a Wizard temperature controller. The reacting gases, all certified calibration gas mixtures with helium (Middlesex), were measured by mass flow controllers and mixed prior to the reactor inlet. The mol percentage of SO<sub>2</sub> in the feed gas was typically unity. Water was injected into a heated gas line with a calibrated syringe pump. The experiments were carried out under nearly atmospheric pressure. A cold trap connected at the outlet of the reactor was used to separate and collect the elemental sulfur and water from the product gas stream. The reactants and products were analyzed by an on-line HP5880A gas chromatograph (GC) equipped with a thermal conductivity detector (TCD). A 1/8 in. OD  $\times$  6 ft. long Teflon column packed with Porapak QS was used to separate CH<sub>4</sub>, CO, CO<sub>2</sub>, COS, CS<sub>2</sub>, H<sub>2</sub>S and SO<sub>2</sub>.

The following notations are used throughout the paper:

$$R = \frac{\text{CH}_{4\text{in}}}{\text{SO}_{2\text{in}}}$$

$$X\text{-SO}_2 = \frac{(\text{SO}_{2\text{in}} - \text{SO}_{2\text{out}})}{\text{SO}_{2\text{in}}}$$

$$Y\text{-[S]} = \frac{\text{Sulfur}_{\text{out}}}{\text{SO}_{2\text{in}}}$$

$$S = \frac{Y\text{-[S]}}{X\text{-SO}_2}$$

where  $\text{CH}_{4\text{in}}$  and  $\text{SO}_{2\text{in}}$  are mol percentages of  $\text{CH}_4$  and  $\text{SO}_2$  in the feed gas, and  $\text{Sulfur}_{\text{out}}$  and  $\text{SO}_{2\text{out}}$  are mol percentages of elemental sulfur and  $\text{SO}_2$  in the effluent gas, respectively. Typically,  $\text{Sulfur}_{\text{out}}$  was determined by subtracting the mol percentages of  $\text{H}_2\text{S}$  in the effluent gas from  $\text{SO}_{2\text{in}} - \text{SO}_{2\text{out}}$ . The definitions of  $X\text{-SO}_2$  and  $Y\text{-[S]}$  are based on a constant molar gas flow rate through the catalyst bed. This assumption is valid since the mole fraction of reactants, i.e.,  $\text{SO}_2$  and  $\text{CH}_4$ , in the feed gas is  $<1\text{--}3\%$ .  $\text{H}_2\text{S}$  was the only sulfur compound detected in the effluent gas stream other than elemental sulfur. Occasionally, a gravimetric measurement was used to determine the amount of sulfur collected in the trap.  $X\text{-SO}_2$ ,  $Y\text{-[S]}$  and  $S$  denote the conversion of  $\text{SO}_2$ , sulfur yield, and selectivity to elemental sulfur, respectively.

### 3.2. Temperature-programmed reduction (TPR) experiments

Temperature-programmed reduction (TPR) of the as-prepared catalysts ( $720^\circ\text{C}$ -calcined) in powder form ( $<150\ \mu\text{m}$ ) in a  $\text{CH}_4/\text{He}$  gas mixture was carried out in a Cahn TG 121 thermogravimetric analyzer (TGA). The catalysts were preheated to  $500^\circ\text{C}$  in a  $5\%\text{O}_2/\text{He}$  mixture ( $50\ \text{cm}^3\ \text{min}^{-1}$  (STP)) for 30 min. After cooling down to room temperature in the  $\text{O}_2/\text{He}$  mixture followed by He purge, the samples were heated in a  $5\%\text{CH}_4/\text{He}$  mixture ( $150\ \text{cm}^3\ \text{min}^{-1}$  (STP)) at a heating rate of  $10^\circ\text{C}\ \text{min}^{-1}$  to  $750^\circ\text{C}$ , while monitoring the catalyst weight change in the TGA.

TPR of pre-sulfated catalysts was conducted in a packed-bed reactor with on-line mass spectrometry. For this study, 150 mg catalyst ( $720^\circ\text{C}$ -calcined) was loaded into the quartz reactor. The catalyst was preheated to  $400^\circ\text{C}$  in He and stabilized for 30 min before the introduction of  $1\%\ \text{SO}_2/\text{He}$  gas mixture

( $50\ \text{cm}^3\ \text{min}^{-1}$  (STP)). After 30 min in this gas stream, the reactor was cooled down in the same gas to room temperature. The catalyst was then purged with He and heated in a  $2\%\ \text{CH}_4/\text{He}$  mixture ( $50\ \text{cm}^3\ \text{min}^{-1}$  (STP)) at a heating rate of  $10^\circ\text{C}\ \text{min}^{-1}$  to  $750^\circ\text{C}$ . The effluent gas was analyzed by mass spectrometer (MS) using a quadrupole residual gas analyzer (MKS-model RS-1). The experimental operation variables in the TPR tests were chosen to satisfy a value of the parameter  $P = \beta S_0 / VC_0 < 20$  K as recommended by Malet and Caballero [18]. In this expression,  $S_0$  is the initial amount of reducible species,  $V$  the total volumetric flow rate,  $C_0$  the initial reductant concentration in the feed gas and  $\beta$  is the heating rate. In addition to pre-sulfated catalysts, a few TPR tests of the as-prepared catalysts were also conducted in the reactor/MS system, following the same pretreatment as that used in the TGA.

### 3.3. Isothermal $\text{SO}_2$ uptake and reduction experiments in the TGA

Tests to measure the  $\text{SO}_2$  uptake capacity of the as-prepared catalysts ( $720^\circ\text{C}$ -calcined) and the reducibility of pre-sulfated catalysts at constant temperature were conducted in the Cahn 121 TGA. A sample of 4–5 mg was loaded into a quartz pan. The temperature was raised to a given value in a flow of He ( $600\ \text{cm}^3\ \text{min}^{-1}$  (STP)) and after the weight was stabilized, a  $1\%\ \text{SO}_2/\text{He}$  gas mixture ( $600\ \text{cm}^3\ \text{min}^{-1}$  (STP)) was switched on for 30 min. This was followed by a gas mixture of  $4\%\ \text{CH}_4/\text{He}$  ( $600\ \text{cm}^3/\text{min}^{-1}$  (STP)). Data were acquired every second for the first 5 min and every 10 s thereafter during the  $\text{SO}_2$  uptake and  $\text{CH}_4$  reduction periods. The  $\text{SO}_2$  uptake curves are plotted as relative weight change per initial unit surface area,  $(\Delta W/W_0)/\text{SA} \times 100\%$ , versus temperature, in which  $\Delta W$  represents the weight change due to uptake of  $\text{SO}_2$ , and  $W_0$  and  $\text{SA}$  are the initial weight and total surface area of the sample, respectively. Fresh materials were used for  $\text{SO}_2$  uptake at each temperature. The isothermal reduction curves are plotted as  $(1 - \text{conversion}) \times 100\%$  versus time, in which conversion is defined as  $(\Delta W/W_s)$ , where  $\Delta W$  is the sample weight drop due to reduction, and  $W_s$  is the sample weight change at the end of sulfation, i.e., the

SO<sub>2</sub> uptake. The reduction rate is defined as follows:

$$R = \frac{\Delta W}{W_i \Delta t}$$

where  $\Delta W$  and  $W_i$  denote, respectively, the weight change in a time interval  $\Delta t$  and the sulfated sample weight at the onset of reduction.

## 4. Results and discussion

### 4.1. Catalyst characterization

The catalysts studied in this work, their surface area and the surface composition of selected samples are shown in Table 1. The XRD pattern of CeO<sub>2</sub> prepared by the urea gelation/coprecipitation technique identified only the fluorite oxide-type structure. For the La-doped ceria with La up to 20 at.%, the XRD pattern did not show separate La<sub>2</sub>O<sub>3</sub> phases. However, the CeO<sub>2</sub> reflections were shifted to lower angle ( $2\theta$ ) with increasing amount of La dopant (Fig. 1 (a)), suggesting oxide solid solution formation, in agreement with previous work in this lab [15]. Fig. 1 (b) shows the XRD patterns of as prepared 5% Cu–Ce(La)Ox and 5% Ni–Ce(La)Ox and used samples in the SO<sub>2</sub> + CH<sub>4</sub> reaction gas mixture. Only the fluorite oxide-type structure was identified on these samples. From other work carried out in this lab [14,15,19], no separate CuO or NiO phases are detected by XRD in ceria samples containing less than 15 at.% Cu or 5 wt.% Ni. STEM/JEDS analyses of as prepared Cu–Ce(La)Ox [14,15] and Ni–Ce(La)Ox [20] showed that at low metal content (<10 at.%), copper or nickel oxide was uniformly dispersed within the CeO<sub>2</sub> matrix as clusters or small particles. At higher metal content, CuO or NiO were identified by XRD and STEM/JEDS [14,15,19,20]. No mixed oxide phases, such as La<sub>2</sub>NiO<sub>4</sub>, were detected by XRD.

### 4.2. Catalyst activity/selectivity tests

The absence of homogenous reactions was verified by passing the 1% SO<sub>2</sub>–0.5% CH<sub>4</sub>–He feed gas mixture into the reactor loaded with quartz wool instead of catalyst. No reaction took place up to 750°C. In other tests, the effect of catalyst prereduction by CO

or H<sub>2</sub> was examined. The SO<sub>2</sub>–CH<sub>4</sub> mixture was also introduced at temperatures lower than 550°C to check the effect of presulfation since sulfates are believed to limit the reaction at low temperatures. No significant effect of pretreatment on the steady state performance of the catalysts was found. However, the steady state conversion would be reached faster at low temperature without any catalyst pretreatment. Therefore, most experiments were conducted with direct introduction of the reactant gas mixture over the catalyst at the temperature of 550°C. The temperature was raised in steps of about 50°C after operating for 2–3 h under steady-state at each temperature point in the light-off experiments. Occasionally, one or two temperatures were checked in the fall-off mode to identify potential hysteresis phenomena as well as to check for catalyst deactivation. No hysteresis was found in these tests.

As shown in Fig. 2, CeO<sub>2</sub> and Ce(La)Ox are active catalysts for the SO<sub>2</sub> reduction by CH<sub>4</sub>. The reaction light-off temperature was about 600°C with a stoichiometric feed gas composition. Over the 650°C-calcined ceria (Fig. 2 (a)), 90% SO<sub>2</sub> conversion and 80% sulfur yield were measured at 700°C at a contact time of 0.36 g s cm<sup>-3</sup> (STP) (S.V.~20,000 h<sup>-1</sup>). Catalysts with a high content of La dopant (>10 at.%), which is known to produce La enrichment of the ceria surface [21], were found to be less active than ceria. However, Ce(La)Ox catalysts containing a small amount of La dopant (4–10 at.%) were found to have better resistance to sintering in air or in the reaction atmosphere than undoped ceria, due to a lower rate of crystallite growth [22,23]. These showed slightly higher activity than undoped ceria after calcination at 750°C (Fig. 2 (b)). There is considerable difference in the surface area of the respective samples (Table 1). Again, the presence of excess La (20 at.%) in ceria resulted in inferior performance. In many other tests, we found that there was no significant difference between a La dopant level of 4.5 at.% and 10 at.%. Therefore, most of the catalysts reported here were doped with ~4.5 at.% La and are denoted as Ce(La)Ox throughout the paper. The dopant level in all materials is expressed in atomic metal percent, as La/(La + Ce) × 100%.

The effect of adding a small amount of a transition metal into the Ce(La)Ox catalysts was studied with copper or nickel addition. The addition of 5 at.% Ni or Cu had a negligible effect on the activity of Ce(La)Ox under dry conditions, as shown in Fig. 3.

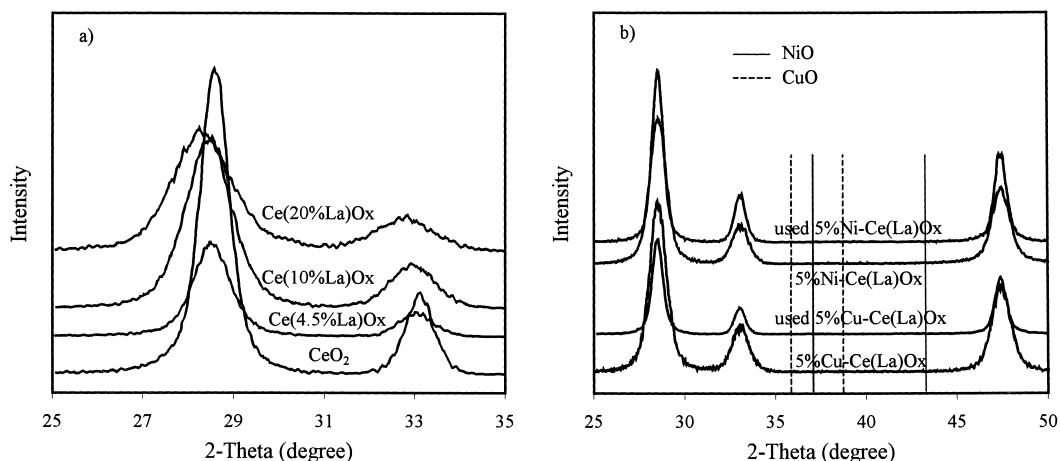


Fig. 1. XRD patterns of ceria-based catalysts, (a) as prepared (after 650°C calcination) CeO<sub>2</sub> and La-doped ceria, (b) 5% Cu–Ce(La)Ox and 5% Ni–Ce(La)Ox, before and after use (in 1% SO<sub>2</sub>–2% CH<sub>4</sub>–He from 550–720°C for a total of 12 h).

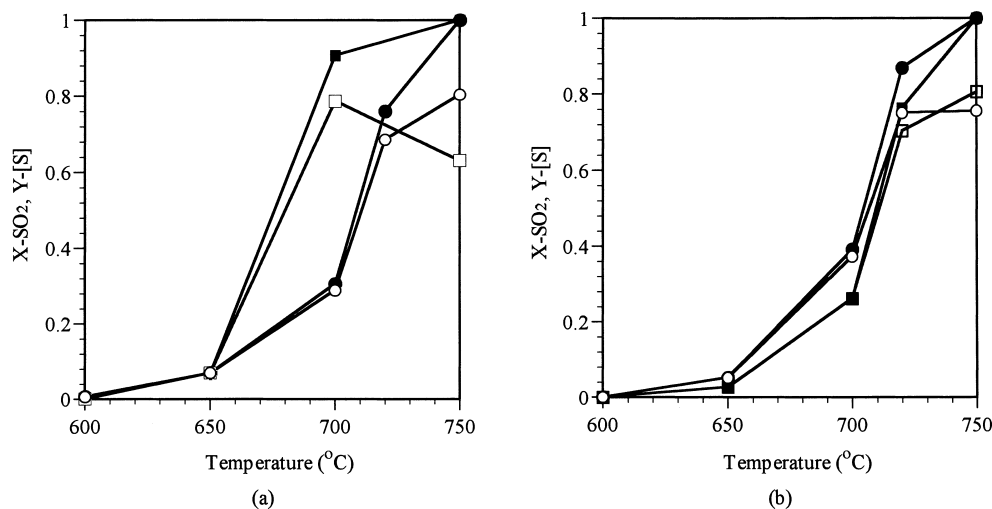


Fig. 2. SO<sub>2</sub> conversion and sulfur yield curves in the SO<sub>2</sub> reduction by CH<sub>4</sub> over CeO<sub>2</sub> and Ce(La)Ox catalysts (1% SO<sub>2</sub>–0.5% CH<sub>4</sub>–He, 0.36 g s cm<sup>-3</sup>(STP)) (a) 650°C-calcined, (b) 750°C-calcined, (■, □) CeO<sub>2</sub>, (●, ○) Ce(4.5% La)Ox, filled symbols: X-SO<sub>2</sub>, open symbols: Y-[S].

However, Cu-modified Ce(La)Ox showed higher selectivity to elemental sulfur under fuel-rich conditions. For example, complete conversion of SO<sub>2</sub> and 83% sulfur yield were obtained at 675°C over a 5% Cu–Ce(La)Ox catalyst at a feed ratio of CH<sub>4</sub>/SO<sub>2</sub> = 2, which is four times the stoichiometric ratio for Reaction (1) (Fig. 3). On the other hand, the selectivity of nickel-modified Ce(La)Ox was a complex function of feed ratio and temperature, as will be discussed below.

The effect of contact time on the SO<sub>2</sub> conversion and sulfur selectivity of 5% Cu–Ce(La)Ox catalyst at the stoichiometric molar feed ratio of CH<sub>4</sub>/SO<sub>2</sub> = 0.5 is illustrated in Fig. 4. The SO<sub>2</sub> conversion of catalysts increased with the contact time, while the selectivity to sulfur at the same SO<sub>2</sub> conversion was not affected by the change of contact time from 0.36 to 1.08 g s cm<sup>-3</sup>(STP). Also, the selectivity to sulfur remained high (>80%) at all conditions. Similar results were obtained at other CH<sub>4</sub>/SO<sub>2</sub> ratios.

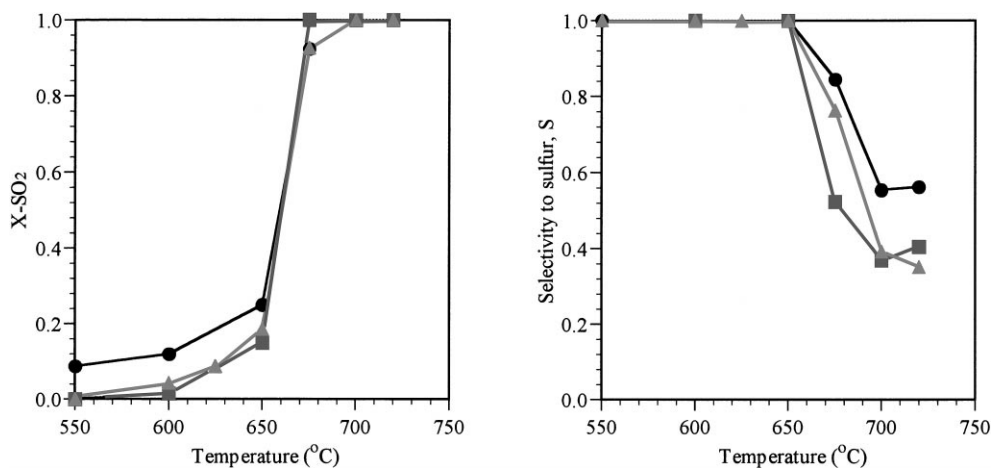


Fig. 3. Effect of catalyst composition on the light-off and sulfur selectivity of the  $\text{SO}_2$  reduction by  $\text{CH}_4$  over ceria-based catalysts ( $720^\circ\text{C}$ -calcined) ( $1\% \text{SO}_2$ - $2\% \text{CH}_4$ -He,  $0.18 \text{ g s cm}^{-3}$  (STP)), (■) Ce(La)Ox, (●) 5% Cu-Ce(La)Ox, (▲) 5% Ni-Ce(La)Ox.

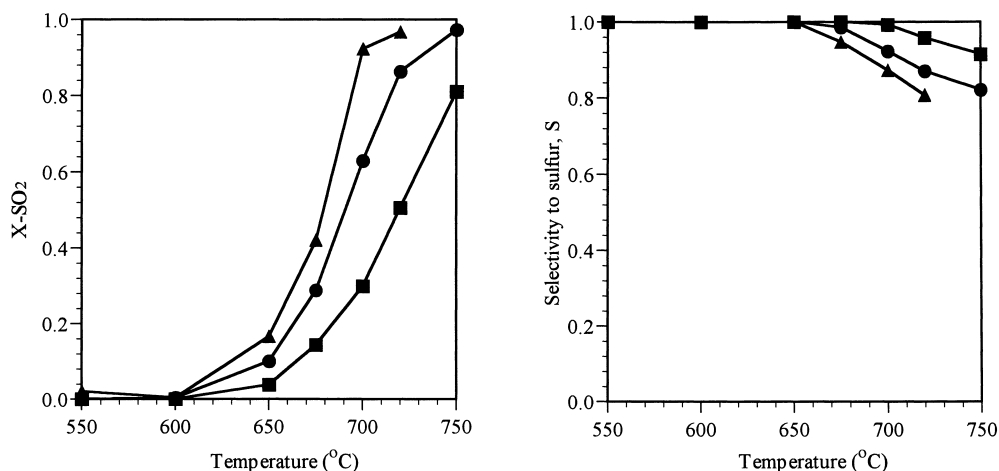


Fig. 4. Effect of contact time on the light-off and sulfur selectivity of the  $\text{SO}_2$  reduction by  $\text{CH}_4$  over a 5% Cu-Ce(La)Ox catalyst ( $720^\circ\text{C}$ -calcined) (■)  $0.36 \text{ g s cm}^{-3}$  (STP), (●)  $0.72 \text{ g s cm}^{-3}$  (STP), (▲)  $1.08 \text{ g s cm}^{-3}$  (STP) ( $1\% \text{SO}_2$ - $0.5\% \text{CH}_4$ -He).

Furthermore, in low  $\text{SO}_2$ -conversion ( $\sim 10\%$ ) experiments over the whole temperature range and with  $\text{CH}_4/\text{SO}_2$  ratio =  $0.5$ – $1.5$ , no  $\text{H}_2\text{S}$ ,  $\text{COS}$  or  $\text{CS}_2$  were observed in the effluent gas stream. The only sulfur product was elemental sulfur (collected in the condenser trap). Hence, elemental sulfur is a primary product of Reaction (1).  $\text{H}_2\text{S}$ , formed under certain conditions, is a secondary product. Similar observations were made in  $\text{SO}_2$  reduction by  $\text{CO}$  over this type of catalyst [14–16]. The redox reaction mechanism can be invoked to explain these findings.

Fig. 5 shows the effect of the molar feed ratio of methane to sulfur dioxide on the  $\text{SO}_2$  conversion and sulfur selectivity of the 5% Cu-Ce(La)Ox catalyst. The higher the ratio of  $\text{CH}_4$  to  $\text{SO}_2$ , the higher the  $\text{SO}_2$  conversion and the lower the catalyst selectivity to sulfur, even though no decrease of selectivity was found below  $650^\circ\text{C}$ . These results indicate that the reaction has a positive dependence on methane; hence by using excess methane we can lower the reaction temperature, keeping both high  $\text{SO}_2$  conversion and sulfur yield at an optimized level. However, the light-off temperature could not be lowered below

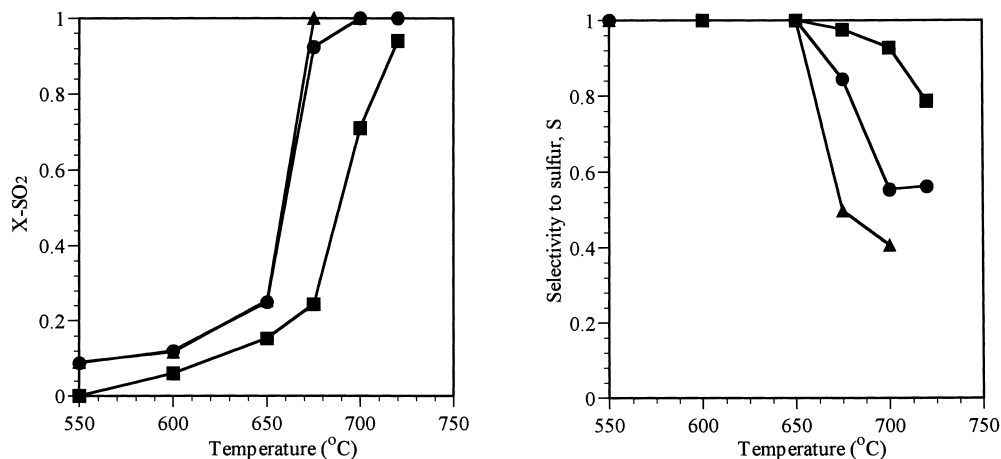


Fig. 5. Effect of the  $\text{CH}_4/\text{SO}_2$  ratio,  $R$ , on the light-off and sulfur selectivity of the  $\text{SO}_2$  reduction by  $\text{CH}_4$  over a 5% Cu–Ce(La)Ox catalyst (720°C-calcined), (■)  $R=1$ , (●)  $R=2$ , (▲)  $R=3$  (1%  $\text{SO}_2$ ,  $0.18 \text{ g s cm}^{-3}$ (STP)).

550°C even after increasing the ratio of  $\text{CH}_4/\text{SO}_2$  to 3. Moreover, undesirable CO as well as  $\text{H}_2\text{S}$  byproducts were detected in the product gas when the feed ratio of  $\text{CH}_4/\text{SO}_2$  was higher than 1 and the reaction temperature was above 650°C.

The production of  $\text{H}_2\text{S}$  and CO at high temperature and fuel-rich conditions suggests that partial oxidation of methane as well as other reactions may also take place over these catalysts. Fig. 6 shows the difference between the  $\text{CH}_4$  consumed and  $\text{CO}_2$  measured in the exit gas as a function of temperature for

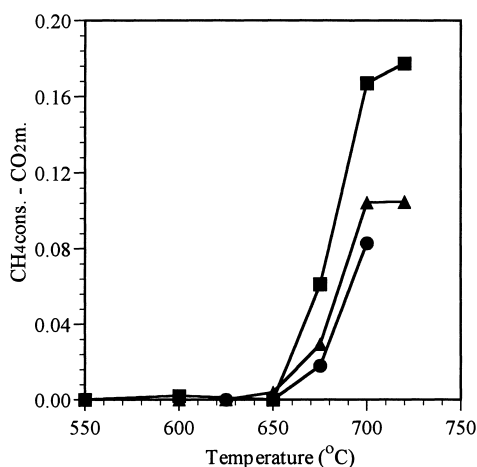
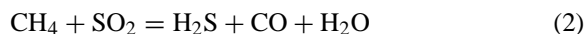
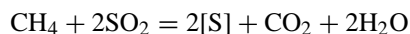


Fig. 6. Effect of catalyst composition on the difference between methane consumption and  $\text{CO}_2$  production in 1%  $\text{SO}_2$ –2%  $\text{CH}_4$ –He,  $0.18 \text{ g s cm}^{-3}$ (STP) (■) Ce(La)Ox, (●) 5% Cu–Ce(La)Ox, (▲) 5% Ni–Ce(La)Ox.

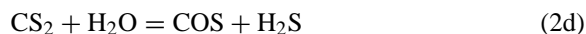
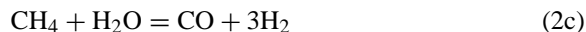
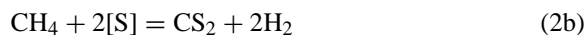
the three catalyst compositions under the conditions of Fig. 3. Under fuel-rich conditions ( $R > 0.5$ ), the measured  $\text{CO}_2$  product could only account for part of the  $\text{CH}_4$  consumption, as shown in Fig. 6, while CO was also detected in the product gases. The amount of CO produced was the difference between the measured  $\text{CH}_4$  consumption and  $\text{CO}_2$  production. Apparently, methane was also consumed to produce CO and  $\text{H}_2$ , as confirmed later by TPR experiments. This can explain the low sulfur yield at high temperature, since the  $\text{H}_2$  produced would further react with surface sulfur to form  $\text{H}_2\text{S}$ .

While a large number of chemical reactions may be written for the  $\text{SO}_2$ – $\text{CH}_4$  reaction system, the above results suggest the following two parallel overall reactions:



As discussed by Nekrich et al. [6], Reaction (1) represents a process with maximum single-stage yield of sulfur and minimum acceptable level of  $\text{SO}_2$  conversion, while Reaction (2) may increase the overall conversion of  $\text{SO}_2$ , but leads to enrichment of the final mixture with  $\text{H}_2\text{S}$  and CO or  $\text{H}_2$  at the expense of elemental sulfur. Alternatively, we may view the first reaction as the complete oxidation of methane by  $\text{SO}_2$ , while in the second reaction, formation of partial oxidation products appear. Although a detailed mech-

anistic study of the formation of H<sub>2</sub>S and CO is outside the scope of this paper, it is worth mentioning the various possible reaction pathways for H<sub>2</sub>S formation, which include:



Carbon formed by methane pyrolysis (Reaction (2a)) can further react with surface oxygen on ceria to form CO. The formation of H<sub>2</sub> and CO at temperatures higher than 600°C over ceria-based catalysts was confirmed by the CH<sub>4</sub>-TPR experiments. Therefore, the reaction of sulfur with partial oxidation products H<sub>2</sub> and CO is a likely reaction pathway for the formation of H<sub>2</sub>S and CO. Trace amounts of CS<sub>2</sub> or COS were observed here and only at high temperatures and long contact times. Thus, CS<sub>2</sub> and COS are rapidly consumed by the hydrolysis reactions (2d) and (2g). No formation of H<sub>2</sub>S, COS, or CS<sub>2</sub> was observed in low SO<sub>2</sub> conversion (~10%) experiments over the whole temperature range and with CH<sub>4</sub>/SO<sub>2</sub> = 0.5–1.5. Thus, elemental sulfur is a primary product of Reaction (1) and does not form H<sub>2</sub>S (or COS) intermediates.

Copper-modified ceria was found to suppress the excess methane consumption and CO production, as shown in Fig. 6. This material has been reported to be a more active catalyst for total oxidation of methane than Ce(La)Ox [15,24]. Therefore, the incorporation of Cu may be used to suppress the partial oxidation of methane at high temperature and, thus, increase the catalyst selectivity to elemental sulfur. The 5% Ni–Ce(La)Ox catalyst was superior to Ce(La)Ox in terms of suppressing excess methane consumption and CO production (Fig. 6), but it similarly favored the production of H<sub>2</sub>S (Fig. 3). As confirmed later, Ni–Ce(La)Ox catalyzes the methane dissociation.

Furthermore, Ni–Ce(La)Ox is very active for methane steam reforming (Reaction (2c)), as shown

in Table 3. Therefore, more H<sub>2</sub>S may be produced at high temperature as a result of H<sub>2</sub> production over Ni–Ce(La)Ox catalysts via the methane dissociation pathway and steam reforming even at low overall methane consumption.

To further examine the above hypothesis, the ceria-based catalysts were tested in fuel-rich methane oxidation with a CH<sub>4</sub>/O<sub>2</sub> molar feed ratio of 2 in the absence of SO<sub>2</sub>. As shown in Fig. 7, Ce(La)Ox is an active catalyst for the total oxidation of methane in the temperature range of 600–750°C. At the contact time of 0.36 g s cm<sup>-3</sup> (STP) (S.V. ~ 20,000 h<sup>-1</sup>), partial oxidation products, CO and H<sub>2</sub>, were observed only at temperatures higher than 650°C. Addition of Cu into Ce(La)Ox suppressed the partial oxidation of methane up to 750°C. In remarkable contrast to these results, the 5% Ni–Ce(La)Ox catalyst was very active for the partial oxidation of methane with >90% methane conversion and high selectivity to syngas (>95%) with H<sub>2</sub>/CO = 2 at T > 650°C. When the space velocity was increased from 20,000 to 60,000 h<sup>-1</sup>, the decrease in methane conversion and CO selectivity over the 5% Ni–Ce(La)Ox catalyst at 650°C was less than 5%. The carbon balance closed to within ±5%. Supported Ni catalysts have been extensively studied for the partial oxidation of methane [25–30]. However, so far there has been little information in the literature on transition metal-modified ceria as a partial oxidation catalyst. This new catalyst is of higher or comparable activity and selectivity to the reported Ni catalysts. A more detailed study of the partial oxidation of methane over Ni-modified Ce(D)O<sub>2</sub> (D = La, Zr) catalysts will be conducted.

From the results of the present work, it appears that the addition of Cu into Ce(La)Ox catalyzes Reaction (1) rather than Reaction (2), thus, improving the sulfur yield. On the other hand, Ni–Ce(La)Ox materials may be more active for Reaction (2) than Ce(La)Ox. The partial oxidation of methane on Ni–Ce(La)Ox may be suppressed in the presence of SO<sub>2</sub> at low temperature. However, at high temperature, the partial oxidation of methane will take place preferentially on the Ni–Ce(La)Ox surface. If this is true, then the ratio of H<sub>2</sub>S produced to CH<sub>4</sub> consumed should be the highest for Ni–Ce(La)Ox catalysts, and the lowest for Cu–Ce(La)Ox. Table 2 lists the ratio of measured H<sub>2</sub>S to CH<sub>4</sub> consumed, H<sub>2</sub>S/CH<sub>4</sub> cons, over Ce(La)Ox and metal-modified ceria at R = 2 and con-

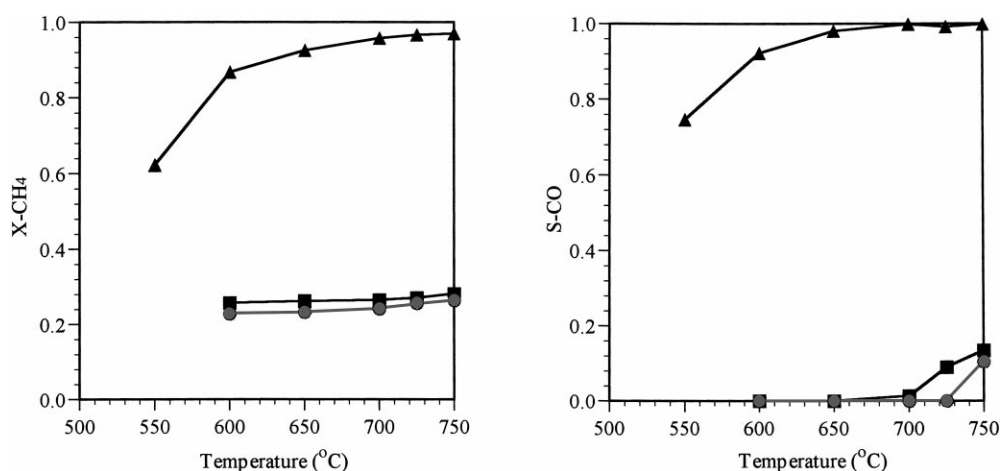


Fig. 7. Partial oxidation of methane over (■) Ce(La)Ox, (●) 5% Cu–Ce(La)Ox, (▲) 5% Ni–Ce(La)Ox catalysts (650°C-calcined) (3% CH<sub>4</sub>–1.5% O<sub>2</sub>–He, 0.36 g s cm<sup>-3</sup> (STP)); X-CH<sub>4</sub> = methane conversion, S-CO = selectivity to CO = yield of CO/(X-CH<sub>4</sub>).

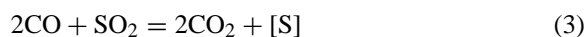
Table 2  
CO and H<sub>2</sub>S produced over ceria-based catalysts under fuel-rich conditions<sup>a</sup>

Sample	H <sub>2</sub> S/CH <sub>4</sub> <sub>cons</sub>			CO/CH <sub>4</sub> <sub>cons</sub>		
	675°C	700°C	720°C	675°C	700°C	720°C
Ce(La)Ox	0.65	0.76	0.73	0.08	0.19	0.20
5%Cu–Ce(La)Ox	0.37	0.55	n.a. <sup>b</sup>	0.04	0.12	n.a. <sup>b</sup>
5%Ni–Ce(La)Ox	0.42	0.84	0.91	0.05	0.13	0.14

<sup>a</sup> Under the conditions of Fig. 3; feed gas composition: 1% SO<sub>2</sub>–2% CH<sub>4</sub>–He; contact time = 0.18 g s cm<sup>-3</sup> (STP).

<sup>b</sup> n.a.: Not available.

tact time = 0.18 g s cm<sup>-3</sup> (STP). These values show that at  $T = 675\text{--}720^\circ\text{C}$ , the H<sub>2</sub>S/CH<sub>4</sub><sub>cons</sub> is decreased in the following order: 5% Ni–Ce(La)Ox > Ce(La)Ox > 5% Cu–Ce(La)Ox. Only at  $T = 675^\circ\text{C}$ , the value of H<sub>2</sub>S/CH<sub>4</sub><sub>cons</sub> over the 5% Ni–Ce(La)Ox catalyst is slightly lower than that of Ce(La)Ox, which may be due to the lower conversion obtained over the nickel-catalyst (Fig. 3). The CO produced from Reaction (2) can further react with SO<sub>2</sub>, providing another pathway for the reduction of SO<sub>2</sub> as follows:



Since this reaction is more favored over the Ni–Ce(La)Ox than the Ce(La)Ox catalysts [14–16,19] the highest ratio of CO produced to CH<sub>4</sub> consumed, CO/CH<sub>4</sub><sub>cons</sub>, is expected to be found over the Ce(La)Ox catalyst. In fact, this was the case, as shown in Table 2. The CO produced from Reaction (2) on Ce(La)Ox may mainly come out unreacted, thus resulting in a higher difference of CH<sub>4</sub> – CO<sub>2</sub>

(i.e. CO) (Fig. 6) and higher CO/CH<sub>4</sub><sub>cons</sub> ratio than for the Ni–Ce(La)Ox catalyst. The sulfur selectivity of Ni–Ce(La)Ox and Ce(La)Ox catalysts under fuel-rich conditions is thus a complex function of the extent of Reactions (1–3).

#### 4.3. Effect of water vapor

In their IR studies of ceria, Li et al. [31] have reported that water vapor may compete with CH<sub>4</sub> for the active surface oxygen species over ceria. Therefore, the presence of water vapor may affect the catalytic performance of ceria-based materials. Fig. 8 shows that the addition of 5% H<sub>2</sub>O in the feed gas greatly affected the performance of Ce(La)Ox by decreasing the SO<sub>2</sub> conversion from 100% to about 10% at 675°C at a contact time of 0.18 g s cm<sup>-3</sup> (STP) and  $R = 2$ . When the water vapor was removed, both the SO<sub>2</sub> conversion and sulfur selectivity of the catalyst were recovered, implying that H<sub>2</sub>O was adsorbed reversibly on the cat-

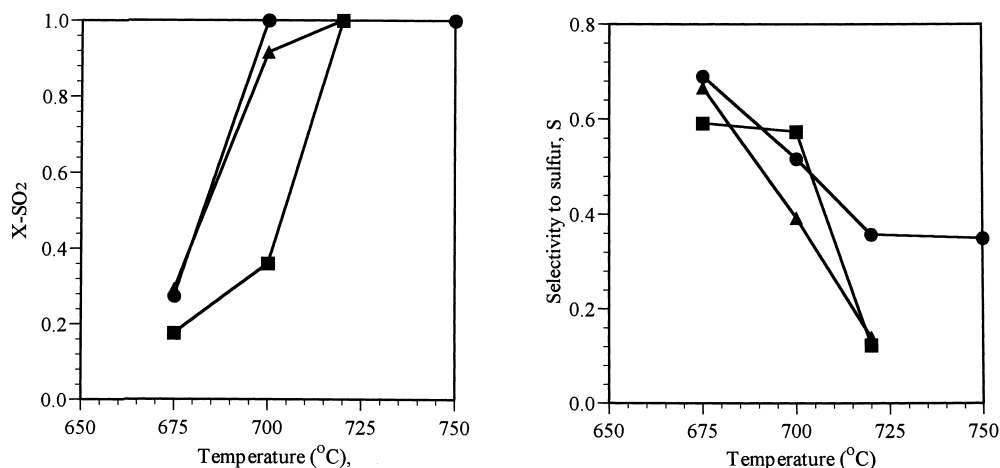


Fig. 8. Effect of water on the light-off and sulfur yield of the SO<sub>2</sub> reduction by CH<sub>4</sub> over ceria-based catalysts (720°C-calcined), (■) Ce(La)Ox, (●) 5% Cu-Ce(La)Ox, (▲) 5% Ni-Ce(La)Ox (1% SO<sub>2</sub>-2% CH<sub>4</sub>-5% H<sub>2</sub>O-He, 0.18 g s cm<sup>-3</sup>(STP)).

alyst surface and that it did not cause any permanent structural change. Thus, upon increasing the temperature, the activity of the catalysts was increased, as shown in Fig. 8. The incorporation of Ni or Cu in ceria enhanced the wet activity of the catalyst and the sulfur yield was increased (Fig. 8). The performance of 5% Cu-Ce(La)Ox catalyst was significantly better than that of 5% Ni-Ce(La)Ox in terms of selectivity.

In the presence of H<sub>2</sub>O, several side reactions can take place over the catalyst and change the product distribution:

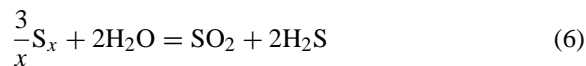
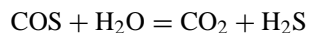
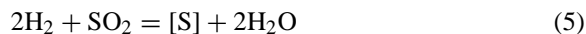
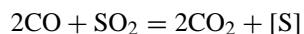
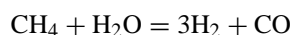


Table 3 shows that Ce(La)Ox and 5% Cu-Ce(La)Ox are not active catalysts for methane steam reforming (Reaction (2c)), while Ni-Ce(La)Ox is an active catalyst for this reaction. Therefore, certain sites for methane activation over Ce(La)Ox and Cu-modified

catalysts may be inhibited by water vapor, while nickel may provide different sites for methane activation. However, the situation becomes more complex in the reaction system of SO<sub>2</sub> + CH<sub>4</sub> + H<sub>2</sub>O. Competitive adsorption of H<sub>2</sub>O and SO<sub>2</sub> may also cause the reduced activity of Ce(La)Ox seen in Fig. 8. It also explains the increase of SO<sub>2</sub> conversion with temperature in the same figure.

As reported by Liu [15] and from separate experiments carried out in our laboratory more recently, the above ceria-based materials are active catalysts for the CO + SO<sub>2</sub> reaction (Reaction (3)), water-gas shift reaction (Reaction (4)), H<sub>2</sub> + SO<sub>2</sub> reaction (Reaction (5)), COS hydrolysis (Reaction (2g)) and the reverse Claus reaction (Reaction (6)). The hydrolysis of COS is almost complete, with 99% of COS hydrolyzed to H<sub>2</sub>S over the temperature range of 250–650°C. Ni- and especially Cu-modified materials are more active catalysts for the water-gas shift reaction than Ce(La)Ox [19]. There is no significant effect of catalyst composition on the CO + SO<sub>2</sub> reaction in the presence of water at temperatures higher than 550°C [15,19]. No data on the wet gas activity/selectivity of ceria-based catalysts for the H<sub>2</sub> + SO<sub>2</sub> reaction are available at the present time. However, through the enhancement of the water-gas shift reaction (Reaction (4)), the equilibrium of the steam reforming reaction (Reaction (2c)) would shift to the right to produce more CO and H<sub>2</sub>, which would further react with SO<sub>2</sub> and surface sulfur. This hypothesis is supported by a much higher produc-

Table 3  
Methane conversion in steam reforming reaction over ceria-based catalysts<sup>a</sup>

Temperature (°C)	Ce(La)Ox	5% Cu–Ce(La)Ox	5% Ni–Ce(La)Ox
550	0	0	0.917
600	0	0	0.965
650	0	0	1.0
700	0.029	0.03	1.0
720	0.059	0.055	1.0

<sup>a</sup> Catalysts were calcined at 720°C; gas composition: 1% CH<sub>4</sub>–5% H<sub>2</sub>O–He; contact time = 0.18 g s cm<sup>-3</sup>(STP).

tion of CO<sub>2</sub> measured in the exit gas under wet than that under dry conditions at the same SO<sub>2</sub> conversion.

Overall, the activity of ceria for the SO<sub>2</sub> reduction by CH<sub>4</sub> under wet conditions is enhanced by the addition of Cu and Ni. However, the presence of nickel is deemed undesirable in view of its high activity for the steam reforming of methane, (Reaction (2c)) (Table 3), and the resulting very low selectivity to elemental sulfur (Fig. 8). On the other hand, the addition of copper enhances both the activity and the sulfur selectivity of Ce(La)Ox under wet gas reaction conditions. Copper does not catalyze the steam reforming of methane (Reaction (2c)) (Table 3). Accordingly, the sulfur selectivity of 5% Cu–Ce(La)Ox under wet conditions (Fig. 8) was very close to that under the corresponding dry conditions (Fig. 3).

#### 4.4. SO<sub>2</sub> uptake experiments in the TGA

Ceria can react with SO<sub>2</sub> over a fairly wide temperature range with or without O<sub>2</sub> to form sulfite or sulfate species [32,33]. The uptake of SO<sub>2</sub> by Ce(La)Ox was studied in the TGA over the temperature range of 170–650°C. At each temperature, a fresh load of catalyst was exposed to the 1% SO<sub>2</sub>/He gas mixture for 30 min. Recent IR studies of CeO<sub>2</sub> sulfation [33] have shown that surface sulfate as well as bulk sulfate can be formed upon exposure of CeO<sub>2</sub> to SO<sub>2</sub> even without O<sub>2</sub> in the gas phase. A large increase in the formation of bulk sulfate was observed above 500°C. However, the thermal stability of bulk cerium sulfate in He was found to be lower than that of surface sulfate. To account for different total surface area of the samples used in the present work, we normalized the SO<sub>2</sub> uptake with the initial surface area of the sample.

The uptake of SO<sub>2</sub> on Ce(La)Ox increased with temperature upto 550°C, as shown in Fig. 9. A steep decrease was observed from 550 to 650°C which is at-

tributed to reduced thermal stability of sulfate species. We observed no weight loss by removing the SO<sub>2</sub> from the feed gas when the temperature was lower than 550°C. Apparently, stable sulfate species were present upto this temperature. At higher temperature, reversible and irreversible adsorption of SO<sub>2</sub> were observed. According to the IR studies of Waqif et al. [33], a large part of the bulk cerium sulfate had decomposed after evacuation at 600°C. In addition, Liu et al. [16] have reported that at a temperature around 550°C, the desorption of SO<sub>2</sub> from copper-modified ceria became significant in the absence of gaseous SO<sub>2</sub>. Thus, bulk sulfate, which is formed above a certain temperature, will decompose in He due to its low thermal stability. Surface sulfate species may decompose at higher temperature. Although it is difficult to differentiate between the decomposition of bulk and surface sulfate in our experiments, the data suggest that a decrease in the overall SO<sub>2</sub> adsorption capacity is caused by the lower thermal stability of sulfate at high temperature.

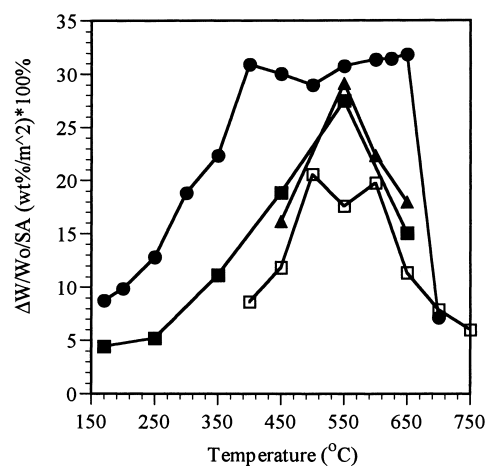


Fig. 9. Variation of SO<sub>2</sub> uptake with temperature. (□) CeO<sub>2</sub>, (■) Ce(La)Ox, (●) 5% Cu–Ce(La)Ox, (▲) 5% Ni–Ce(La)Ox (30 min SO<sub>2</sub> uptake, 1% SO<sub>2</sub>/He, 600 cm<sup>3</sup> min<sup>-1</sup>(STP)).

From Fig. 9, we see that the  $\text{SO}_2$  uptake of  $\text{Ce}(\text{La})\text{Ox}$  is higher than that of  $\text{CeO}_2$ . The incorporation of a small amount of Ni (5 at.%) had a negligible effect on the sulfation of  $\text{Ce}(\text{La})\text{Ox}$ . On the other hand, the addition of 5 at.% Cu changed the  $\text{SO}_2$  adsorption behavior significantly. As shown in Fig. 9, the amount adsorbed was higher for the 5% Cu- $\text{Ce}(\text{La})\text{Ox}$ . The weight increase due to sulfation of the copper oxide in this material would not exceed 1.86 wt.% (corresponding to 5–7.5 wt.%  $\text{m}^{-2}$ , depending on the catalyst amount used), which was calculated by assuming that all the copper in the catalyst existed as cupric oxide fully exposed to  $\text{SO}_2$ . This value is smaller than the difference in  $\text{SO}_2$  uptake between the  $\text{Ce}(\text{La})\text{Ox}$  and 5% Cu- $\text{Ce}(\text{La})\text{Ox}$  samples at  $T > 250^\circ\text{C}$  (Fig. 9), indicating that copper promotes the uptake of  $\text{SO}_2$  by  $\text{Ce}(\text{La})\text{Ox}$ . A plateau in  $\text{SO}_2$  uptake is observed for the Cu-containing sample at 400–650°C in Fig. 9. A similar profile was obtained in the temperature range of 400–600°C after a 90 min-long uptake with a slightly higher weight increase. These results indicate the presence of a sulfate of different thermal stability.

The increased  $\text{SO}_2$  uptake on  $\text{Ce}(\text{La})\text{Ox}$  and Cu- $\text{Ce}(\text{La})\text{Ox}$  catalysts is in line with the higher oxygen storage capacity of these materials compared to that of  $\text{CeO}_2$ . Benedek et al. [34] have reported a promotion effect of Cu on the sulfation of  $\text{CeO}_2$  in mixed CuO- $\text{CeO}_2$  materials used for  $\text{SO}_2$  removal from simulated flue gas streams (0.3%  $\text{SO}_2$ , 3–10%  $\text{O}_2$ ). Accordingly, the sulfation of ceria was increased and also shifted to lower temperature in the presence of CuO. As has been reported in the literature [15,24,35,36] the reducibility and oxygen mobility of ceria are enhanced by the addition of La-dopant or a small amount of a transition metal. This is also shown here in  $\text{CH}_4$ -TPR experiments of the as-prepared catalysts. The enhanced capacity of  $\text{Ce}(\text{La})\text{Ox}$  and Cu- $\text{Ce}(\text{La})\text{Ox}$  for  $\text{SO}_2$  might be due to the higher oxygen supply induced by the dopant and copper, since surface oxygen species are the active sites for  $\text{SO}_2$  adsorption. However, the adsorption behavior of the 5% Ni- $\text{Ce}(\text{La})\text{Ox}$  sample could not be explained in the same way. XPS analysis showed that the surface content of nickel was lower than the bulk concentration (5 or 10 at.%) in Ni- $\text{Ce}(\text{La})\text{Ox}$  catalysts (Table 1). On the other hand, ceria-surface enrichment with copper has been reported by Liu et al. [14,15,21] and found again in this work (Table 1), which supports the

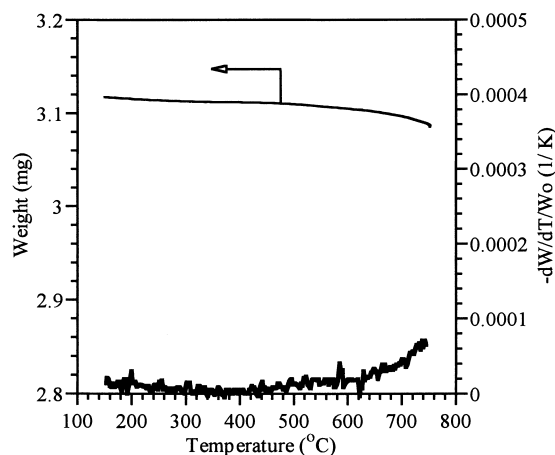


Fig. 10.  $\text{CH}_4$ -TPR profiles of  $\text{Ce}(\text{La})\text{Ox}$  in the TGA (5%  $\text{CH}_4/\text{He}$ ,  $10^\circ\text{C min}^{-1}$ ,  $200 \text{ cm}^3 \text{ min}^{-1}$  (STP)).

argument that a much higher concentration of active oxygen exists on the surface of Cu-modified ceria.

Overall, the  $\text{SO}_2$  uptake experiments have indicated that sulfate species start to decompose at  $\sim 550^\circ\text{C}$ , which is the light-off temperature of the  $\text{CH}_4 + \text{SO}_2$  reaction. The confirmation of this was obtained by studying the stability of pre-sulfated catalysts in methane and by  $\text{CH}_4$ -TPR as described below.

#### 4.5. Reducibility of the as-prepared catalysts

The reducibility of the as-prepared catalysts by  $\text{CH}_4$  was studied in the TGA. Fig. 10 shows the TPR profile of  $\text{Ce}(\text{La})\text{Ox}$  in the 5%  $\text{CH}_4/\text{He}$  gas mixture. The catalyst reduction began at a temperature around  $450^\circ\text{C}$ . In recent literature, oxygen species on ceria have been discussed as sites for methane activation [22,24,31,37]. However, the reactivity of methane with the oxygen species over ceria is lower than that of CO or  $\text{H}_2$ , both of which begin to react with surface oxygen at temperatures below  $400^\circ\text{C}$ . The activation of methane may be limited by the high energy required to break the first C-H bond ( $104 \text{ kcal mol}^{-1}$ ) [37].

In a  $\text{CH}_4$ -TPR experiment of  $\text{Ce}(\text{La})\text{Ox}$  using the reactor/MS system, production of hydrogen and carbon monoxide was observed after the temperature reached  $630^\circ\text{C}$  (Fig. 11). The intensity of each signal is modified by the intensity of He signal and is expressed as  $I/I_0$  in this figure. The formation of  $\text{CO}_2$  begins at lower temperature, coinciding with the onset of de-

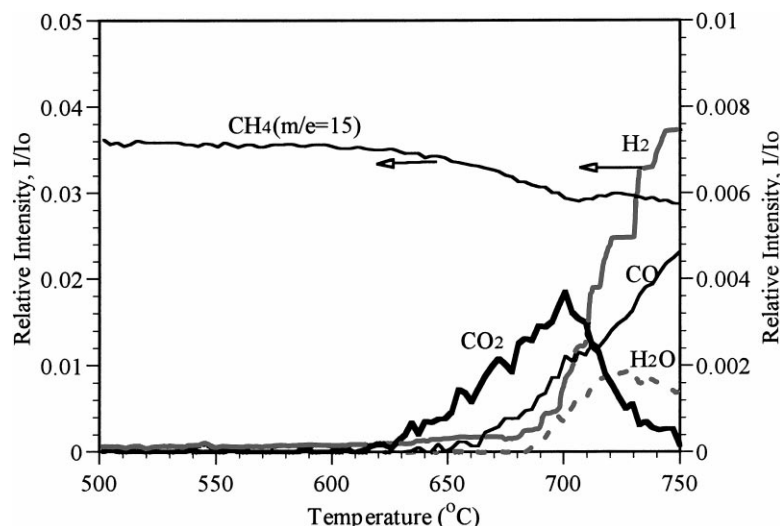


Fig. 11. CH<sub>4</sub>-TPR of Ce(La)Ox in the reactor/MS system (2% CH<sub>4</sub>/He, 10°C min<sup>-1</sup>, 50 cm<sup>3</sup> min<sup>-1</sup> (STP)).

crease of the methane signal. Therefore, the initial interaction of methane is with the surface oxygen of the catalyst, leading to complete oxidation of methane to CO<sub>2</sub> and H<sub>2</sub>O. As the temperature is increased, the catalyst surface is reduced and may contain oxygen vacancies. Partial oxidation of methane into CO and H<sub>2</sub> can then take place over the reduced ceria surface, as has been discussed by Otsuka et al. [38,39].

CH<sub>4</sub>-TPR profiles of metal-modified Ce(La)Ox catalysts obtained in the TGA are shown in Fig. 12. A temperature peak centered at 420°C was observed with Cu–Ce(La)Ox catalysts, which was caused by the addition of copper, and the intensity of the peak was increased with increasing Cu content upto 15 at.%. It has been suggested by Bethke et al. [40] that catalysts containing dispersed CuO nanoparticles are more active for hydrocarbon combustion. Moreover, experiments carried out by Kundakovic et al. [22,24] have identified that copper-modified cerium oxide materials are more reducible and more active catalysts for the complete oxidation of methane than unmodified ceria. With 5% Ni–Ce(La)Ox, a sharp weight decrease appeared in the CH<sub>4</sub>-TPR profile at 510°C (Fig. 12). This was also observed with the 10% Ni–Ce(La)Ox material. In a CH<sub>4</sub>-TPR experiment with the same material carried out in the reactor coupled with the MS, a significant amount of hydrogen was produced around 600°C (Fig. 13). This was attributed to the dissociation of methane on nickel metal. The sharp weight

decrease observed in the TGA over Ni–Ce(La)Ox catalysts was attributed to the reduction of NiO and the support by the hydrogen produced from the decomposition of methane on the freshly formed nickel metal.

After the CH<sub>4</sub>-TPR tests, no color change was observed for Ce(La)Ox and 5%Cu–Ce(La)Ox. On the other hand, 5% Ni–Ce(La)Ox turned black. Carbon deposition during CH<sub>4</sub>-TPR on Ni–Ce(La)Ox was confirmed by subsequent temperature-programmed oxi-

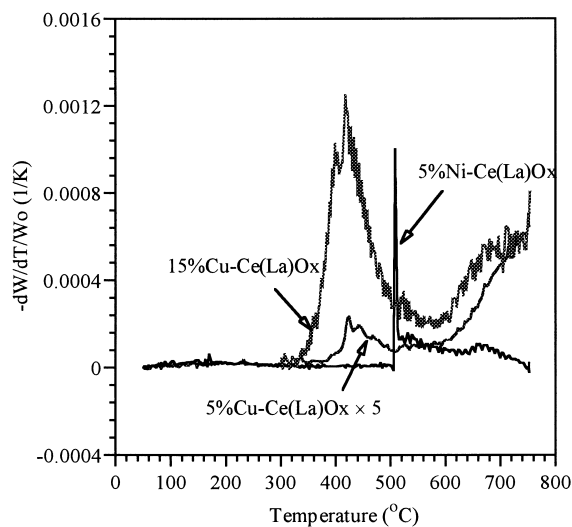


Fig. 12. TPR profiles of Cu- and Ni-modified Ce(La)Ox in 5% CH<sub>4</sub>/He in the TGA (10°C min<sup>-1</sup>, 200 cm<sup>3</sup> min<sup>-1</sup> (STP)).

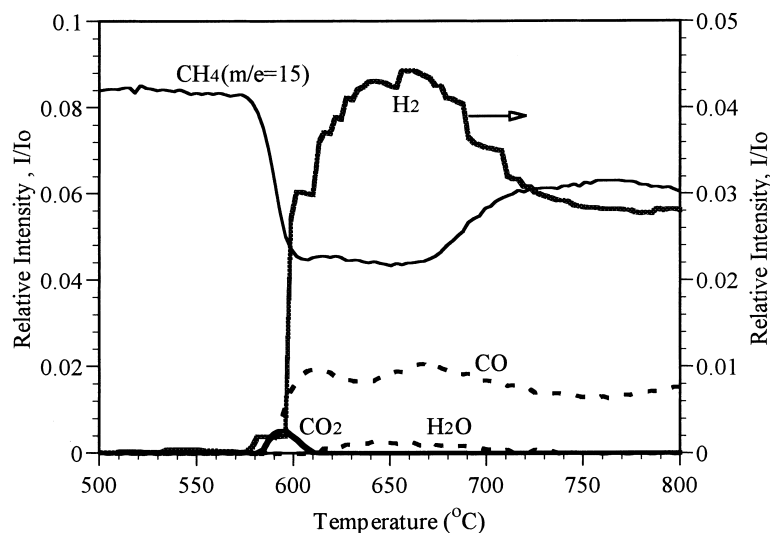


Fig. 13. TPR profiles (reactor/MS) of 5% Ni-Ce(La)Ox in 2% CH<sub>4</sub>/He (10°C min<sup>-1</sup>, 150 mg, 50 cm<sup>3</sup> min<sup>-1</sup>(STP)).

ation carried out in the reactor/MS in which CO<sub>2</sub> formation was observed at temperatures higher than 350°C.

#### 4.6. Reducibility of pre-sulfated catalysts

The catalyst surface may be partially sulfated during the SO<sub>2</sub>-CH<sub>4</sub> reaction. This has been identified already for the CO-SO<sub>2</sub> reaction over this type of catalyst [15,16]. Studying the reducibility of pre-sulfated catalysts has, thus, an important scope for elucidating the SO<sub>2</sub> reduction by CH<sub>4</sub>. CH<sub>4</sub>-TPR experiments of pre-sulfated catalysts were carried out in the reactor with the product gases analyzed by mass spectrometer. For this study, catalysts were pre-sulfated at 400°C, and separate experiments confirmed that SO<sub>2</sub> was adsorbed on the catalysts and that thermally stable sulfate species were also formed. As shown in Fig. 14 (a), oxygen started to desorb at 600°C before the elution of SO<sub>2</sub>. This oxygen desorption was not observed in the CH<sub>4</sub>-TPR experiments of fresh catalysts. Therefore, it may be attributed to the decomposition of sulfate species. The decrease of the methane signal began at the same time as the O<sub>2</sub> elution at 600°C. This temperature was almost the same as the corresponding temperature of the onset of thermal decomposition of sulfate species in He, as shown by the He-TPD of

the Ce(La)Ox material (Fig. 14(d)). Moreover, similar results were obtained in CH<sub>4</sub>-TPR and He-TPD experiments of the pre-sulfated Ce(La)Ox material carried out in the TGA, i.e., the catalyst weight started to decrease at the same temperature. Therefore, we conclude that methane activation over these catalysts can occur only after partial decomposition of the sulfated surface. Partial oxidation products, H<sub>2</sub> and CO, were also detected on the partially sulfated catalyst at a higher temperature, about 680°C (Fig. 14 (a)), at which point a significant amount of H<sub>2</sub>S was formed under reaction conditions (Fig. 3). Methane may react with the lattice oxygen at high temperatures, producing partial oxidation products. Under fuel-rich reaction conditions, the H<sub>2</sub> produced would react with elemental sulfur to form H<sub>2</sub>S and decrease the catalyst selectivity to elemental sulfur as previously discussed. The CO produced would be largely emitted unreacted depending on the reaction conditions.

The CH<sub>4</sub>-TPR profiles of pre-sulfated catalysts were different for metal-modified ceria materials, as shown in Fig. 14 (a-c). The desorption temperatures of O<sub>2</sub> and SO<sub>2</sub> as well as the elution temperature of CO<sub>2</sub> were lower for the 5% Ni-Ce(La)Ox catalyst (Fig. 14 (c)) than for Ce(La)Ox (Fig. 14 (a)), suggesting an increase of the reducibility of pre-sulfated catalysts by the incorporation of nickel. There is no significant shift in the temperature of H<sub>2</sub> and CO

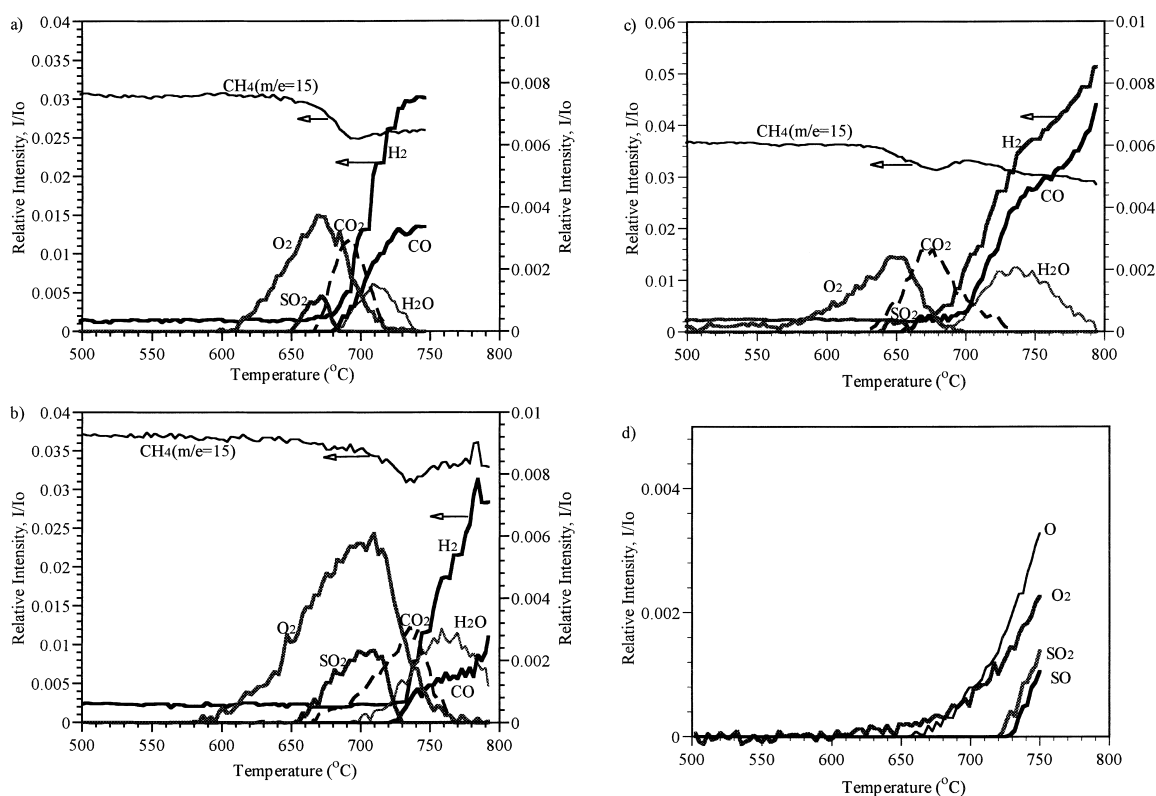


Fig. 14. TPR profiles (reactor/MS) of pre-sulfated catalysts in 2%  $\text{CH}_4/\text{He}$ , (a)  $\text{Ce}(\text{La})\text{Ox}$ , (b) 5%  $\text{Cu-Ce}(\text{La})\text{Ox}$ , (c) 5%  $\text{Ni-Ce}(\text{La})\text{Ox}$ , (d) He-TPD of pre-sulfated  $\text{Ce}(\text{La})\text{Ox}$ , all catalysts pre-sulfated with 1%  $\text{SO}_2/\text{He}$  at  $400^\circ\text{C}$  for 30 min ( $10^\circ\text{C min}^{-1}$ , 150 mg,  $50\text{ cm}^3\text{ min}^{-1}$  (STP)).

production for this material from that of  $\text{Ce}(\text{La})\text{Ox}$ , implying that partial oxidation of methane on the pre-sulfated Ni-modified catalysts was suppressed at low temperatures. On the other hand, the evolution of  $\text{H}_2$  and  $\text{CO}$  over 5%  $\text{Cu-Ce}(\text{La})\text{Ox}$  was shifted to a higher temperature (Fig. 14 (b)). This result provides supporting evidence to our assumption that copper suppresses the partial oxidation of methane during the reaction of  $\text{SO}_2 + \text{CH}_4$ , thus increasing the selectivity to elemental sulfur (Reaction 1). No methane activation was observed at temperatures lower than  $550^\circ\text{C}$  over the pre-sulfated catalysts. Deberry et al. [41] reported that  $\text{NiO}$  and  $\text{CuO}$  can form bulk sulfates in the presence of  $\text{SO}_2$  and  $\text{O}_2$  at  $380$  and  $325^\circ\text{C}$ , respectively. Although there is no  $\text{O}_2$  present in the reaction gas mixture of  $\text{CH}_4 + \text{SO}_2$ , stable surface sulfates of  $\text{NiO}$  and  $\text{CuO}$  may still be formed, as  $\text{SO}_2$  adsorbs on these oxides and ceria at low temperature. Previous XPS studies of  $\text{Cu-Ce}(\text{La})\text{Ox}$  catalysts by Liu et al. [15,16] have shown that the working cat-

Table 4

Surface composition of the 10%  $\text{Ni-Ce}(\text{La})\text{Ox}$  catalyst<sup>a</sup>

Element	Before use <sup>b</sup> (at.%)	After use <sup>c</sup> (at.%)
Ni	1.63	2.27
La	1.61	1.10
Ce	23.44	15.89
S	0	6.67
O	73.72	74.07

<sup>a</sup> Determined by XPS.

<sup>b</sup> After air calcination at  $720^\circ\text{C}$ , 3 h.

<sup>c</sup> At  $T = 720^\circ\text{C}$ , in 1%  $\text{SO}_2$ -2%  $\text{CH}_4$ -He;  $0.18\text{ g s cm}^{-3}$ .

alyst comprises  $\text{CuO}$ , sulfide and sulfate as well as cerium oxide and sulfate in the  $\text{CO} + \text{SO}_2$  reacting atmosphere. Along the same line, the XPS surface composition analysis of  $\text{Ni-Ce}(\text{La})\text{Ox}$  catalysts used in fuel-rich  $\text{CH}_4$ - $\text{SO}_2$  mixture (Table 4) still shows an increase of sulfur and oxygen on the surface, indicative of the presence of sulfate species in the working catalyst. Therefore, at low temperatures, stable metal sulfates on the catalyst surface prevent the activation

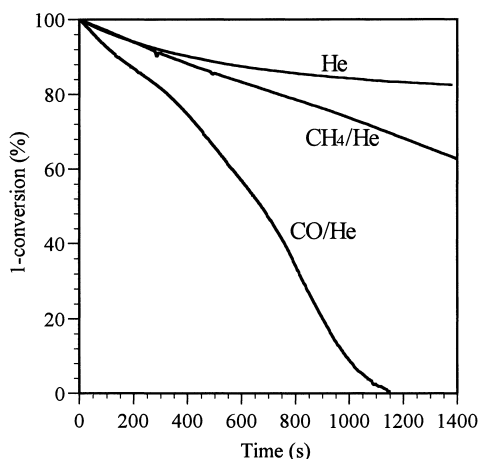


Fig. 15. Reduction/decomposition of pre-sulfated (400°C, 30 mm in 1% SO<sub>2</sub>/He) 5% Cu–Ce(La)Ox at 550°C. Reduction with 4% CH<sub>4</sub>/He or 2% CO/He (600 cm<sup>3</sup> min<sup>-1</sup>(STP)), decomposition in He (600 cm<sup>3</sup> min<sup>-1</sup>(STP)), both in the TGA.

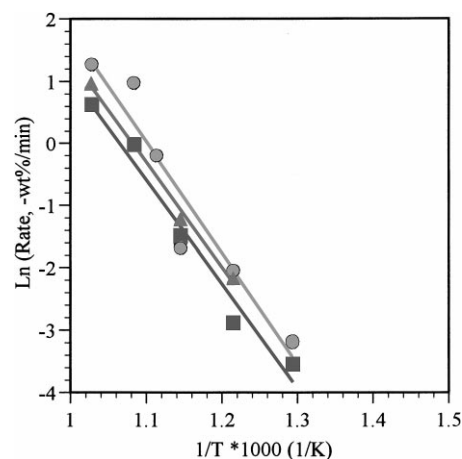


Fig. 16. Arrhenius-type plot for the reduction of presulfated catalysts with methane, (■) Ce(La)Ox, (●) 5% Cu–Ce(La)Ox, (▲) 5% Ni–Ce(La)Ox. Reduction with 4% CH<sub>4</sub>/He (600 cm<sup>3</sup> min<sup>-1</sup>(STP)) in the TGA.

of methane. The activity of the metal-modified ceria catalysts then depends on the thermal stability of the metal sulfate. This is further supported by the data of Fig. 15, which shows the same initial slope for the thermal decomposition profile in He and the reduction profile in CH<sub>4</sub>/He mixtures of the 5% Cu–Ce(La)Ox catalyst at 550°C. The same initial slopes obtained in two different mixtures suggest that the initial rate, i.e., the decomposition of sulfates, is independent of the presence of CH<sub>4</sub>. However, the situation is different in the presence of CO. The reduction with CO is a much faster process, showing a higher rate throughout the reduction period.

The initial rate of reduction, shown as an Arrhenius-type plot in Fig. 16, is similar for Ce(La)Ox and Cu- or Ni-modified catalysts in the temperature range of 500–700°C. The activation energy was  $143 \pm 5 \text{ kJ mol}^{-1}$ , the same for all three catalysts. Thus, the key step of the reaction between CH<sub>4</sub> and pre-sulfated catalysts may be the same for all catalysts, probably that of the decomposition of sulfates. The reduction of pre-sulfated 15% Cu–Ce(La)Ox with CO had a much higher rate [16] than that with CH<sub>4</sub>. This may be due to the different reactivity (reducibility) of sulfate species in CO and CH<sub>4</sub>. It has been suggested that sulfate species could be reduced by CO [15,16], while the above results indicate that the activation of methane is limited by sulfate decomposition.

## 5. Conclusions

La-doped ceria is a highly active catalyst for the SO<sub>2</sub> reduction by CH<sub>4</sub> at temperatures above 550°C. Strong adsorption of SO<sub>2</sub> forms surface sulfate and inhibits methane activation at temperatures below 550°C. The reaction between SO<sub>2</sub> and CH<sub>4</sub> begins on a partially sulfated catalyst. Thus, the light-off temperature of ceria-based catalysts depends on the thermal stability of the sulfates. The activation of methane may involve surface oxygen species and partially reduced metal oxide sites. Two independent reactions are proposed and used to explain the catalytic performance of ceria-based oxides. The addition of the transition metals nickel and copper has a different effect on sulfur selectivity under fuel-rich conditions, through catalyzing different pathways of methane activation. Copper catalyzes the complete oxidation of methane by SO<sub>2</sub>, which leads to elemental sulfur production. In contrast, nickel provides extra sites for methane dissociation at high temperature and gives low yields of elemental sulfur under fuel-rich conditions. In the presence of water vapor, Ce(La)Ox is a poor catalyst. However, Cu–Ce(La)Ox catalyst is still a very active and selective catalyst. With proper further development, this class of catalysts offers promise for practical application to sulfur recovery from various SO<sub>2</sub>-laden gas streams.

## Acknowledgements

This work was financially supported by the US Department of Energy under Contract No. DE-AC-95PC95252 to Arthur D. Little, Inc., and a subcontract to Tufts University.

## References

- [1] S.W. Young, *Trans. Am. Inst. Chem. Eng.* 8 (1915) 81.
- [2] J. J. Helstrom, G.A. Atwood, *Ind. Eng. Chem. Process Des. Dev.* 17 (1978) 114.
- [3] J. Sarlis, D. Berk, *Ind. Eng. Chem. Res.* 27 (1988) 1951.
- [4] D.J. Mulligan, D. Berk, *Ind. Eng. Chem. Res.* 28 (1989) 926.
- [5] T.S. Wiltowski, K. Sangster, W.S. O'Brien, *J. Chem. Tech. Biotech.* 7 (1996) 204.
- [6] E.M. Nekrich, A.N. Kontsevaya, G.F. Ganzha, *J. of Appl. Chem. of U.S.S.R.* 51 (1978) 517.
- [7] D.J. Mulligan, D. Berk, *Ind. Eng. Chem. Res.* 31 (1992) 119.
- [8] J. Sarlis, D. Berk, *Chem. Eng. Comm.* 140 (1996) 73.
- [9] J.J. Yu, Q. Yu, Y. Jin, S.G. Chang, *Ind. Eng. Chem. Res.* 36 (1997) 2128.
- [10] V.A. Zazhigalov, S. V Gerei, M. Rubanik, *Kinet. Katal.* 4 (1975) 967.
- [11] T. Chivers, J.B. Hyne, C. Lau, *Int. J. Hydrogen Energy* 5 (1980) 499.
- [12] S. C Moffat, A.A. Adesina, *Catal. Lett.* 37 (1996) 167.
- [13] M.M. Akhmedov, G.B. Shakhtakhtinskii, A.I. Agaev, S.S. Gezalov, *Zhurnal Prikladnoi Khimii* 59 (1986) 504.
- [14] W. Liu, A.F. Sarofim, M. Flytzani-Stephanopoulos, *Appl. Catal. B* 4 (1994) 167.
- [15] W. Liu, Sc. D. Thesis, Massachusetts Institute of Technology, 1995.
- [16] W. Liu, C. Wadia, M. Flytzani-Stephanopoulos, *Catal. Today* 28 (1996) 391.
- [17] Y. Amenomiya, A. Emesh, K. Oliver, G. Pleizer, in: M Philips, M. Ternan, (Eds.), *Proc. 9th Int. Cong. Catal., Chemical Institute of Canada, Ottawa, Canada, 1988*, p. 634.
- [18] P. Malet, A.J. Caballero, *Chem. Soc. Faraday Trans.* 4(7) (1988) 2369.
- [19] Y. Li, MS Thesis, Tufts University, 1999.
- [20] T. Zhu, Ph.D. Thesis, Tufts University, in progress.
- [21] W. Liu, M. Flytzani-Stephanopoulos, *J. Catal.* 153 (1995) 304.
- [22] L. Kundakovic, M. Flytzani-Stephanopoulos, *Appl. Catal. A* 171 (1998) 13.
- [23] M. Pijolat, M. Prin, M. Soustelle, *Solid State Ionics* 63–65 (1993) 781.
- [24] L. Kundakovic, Ph.D. Thesis, Tufts University, 1998.
- [25] M. Prettre, C. Eichner, M. Perrin, *Trans. Faraday Soc.* 43 (1964) 335.
- [26] G.R. Gavalas, C. Phichitkul, G.E. Voecks, *J. Catal.* 88 (1984) 54.
- [27] D. Dissanayake, M.P. Rosynek, K.C.C. Kharas, J.H. Lunsford, *J. Catal.* 132 (1991) 117.
- [28] V.R. Choudhary, A.M. Rajput, V.H. Rane, *J. Phys. Chem.* 96 (1992) 8686.
- [29] O. Yamazaki, T. Nozaki, K. Omata, K. Fujimoto, *Chem. Lett.* (1992) 1953.
- [30] Z.L. Zhang, X.E. Verykios, *J. Chem. Soc., Chem. Commun.* (1995) 71.
- [31] C. Li, Q. Xin, *J. Phys. Chem.* 96 (1992) 7714.
- [32] S. Lundgren, G. Spiess, O. Hjortsberg, E. Jobson, I. Gottberg, G. Smedler, *Stud. Surf. Sci. Catal.* 96 (1995) 763.
- [33] M. Waqif, P. Bazin, O. Saur, J.C. Lavalley, G. Blanchard, O. Touret, *Appl. Catal. B* 11 (1997) 193.
- [34] K. Benedek, M. Flytzani-Stephanopoulos, Cross-Flow, Filter-Sorbent-Catalyst for Particulate, SO<sub>2</sub> and NO<sub>x</sub> Control, Final Report to the US Department of Energy, Contract No. 22-89PC898O5, May 1994.
- [35] W. Liu, M. Flytzani-Stephanopoulos, *Chem. Eng. J.* 64 (1996) 283.
- [36] G. Wrobel, C. Lamonier, A. Bennani, A. D'Huysser, A. Aboukais, *J. Chem. Soc., Faraday Trans.* 92 (1996) 2001.
- [37] R.O. Long, Y.P. Huang, H.L. Wan, *J. Raman Spectroscopy* 28 (1997) 29.
- [38] K. Otsuka, T. Ushiyama, I. Yamanaka, *Chem. Lett.* (1993) 1517.
- [39] K. Otsuka, E. Sunada, T. Ushiyama, I. Yamanaka, *Stud. Surf. Sci. Catal.* 107 (1997) 531.
- [40] K.A. Bethke, M.C. Kung, B. Yang, M. Shah, D. Alt, C. Li, H.H. Kung, *Catal. Today* 26 (1995) 169.
- [41] D.W. Deberry, K.J. Sladek, *Can. J. Chem. Eng.* 49 (1971) 781.